Rapid and Reliable Thickness Identification of Two-Dimensional Nanosheets Using Optical Microscopy

Hai Li,[†,§] Jumiati Wu,[†,§] Xiao Huang,[†] Gang Lu,[†] Jian Yang,[†] Xin Lu,[‡] Qihua Xiong,[‡,∥] and Hua Zhang[†,*]

[†]School of Materials Science and Engineering, Nanyang Technological University, 50 Nanyang Avenue, Singapore 639798 and [‡]Division of Physics and Applied Physics, School of Physical and Mathematical Sciences, Nanyang Technological University, 21 Nanyang Link, Singapore 637371. [∥]NOVITAS, Nanoelectronics Centre of Excellence, School of Electrical and Electronic Engineering, Nanyang Technological University, Singapore 639798. [§]These authors contributed equally to this work.

ABSTRACT The physical and electronic properties of ultrathin two-dimensional (2D) layered nanomaterials are highly related to their thickness. Therefore, the rapid and accurate identification of single- and few- to multilayer nanosheets is essential to their fundamental study and practical applications. Here, a universal optical method has been developed for simple, rapid, and reliable identification of single- to quindecuple-layer (1L−15L) 2D nanosheets, including graphene, MoS_2, WSe_2, and TaS_2, on Si substrates coated with 90 or 300 nm SiO_2. The optical contrast differences between the substrates and 2D nanosheets with different layer numbers were collected and tabulated, serving as a standard reference, from which the layer number of a given nanosheet can be readily and reliably determined without using complex calculation or expensive instrument. Our general optical identification method will facilitate the thickness-dependent study of various 2D nanomaterials and expedite their research toward practical applications.

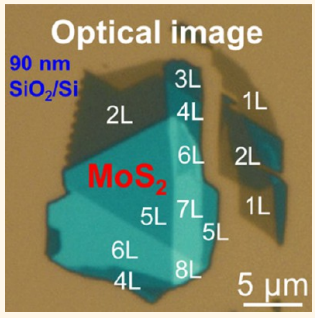

KEYWORDS: thickness identification · optical microscopy · 2D nanosheets · graphene · MoS_2 · WSe_2 · contrast difference

Two-dimensional (2D) layered nanomaterials, such as graphene and transition metal dichalcogenides (TMDs, *e.g.*, MoS_2, WSe_2, and TaS_2),[1−10] have attracted much attention in recent years due to their novel optical, electronic, mechanical, and magnetic properties in contrast to their bulk crystals. Currently, mechanical exfoliation is still one of the most efficient ways to obtain high-quality, atomically thin nanosheets of 2D layered nanomaterials.[1,3−7] However, this technique produces not only single- and few- to multilayer nanosheets but also a large quantity of thicker flakes. It is well-known that the physical and electronic properties of 2D nanomaterials are highly related to their thickness.[3−6,11−17] Therefore, the rapid determination of location and layer number of mechanically exfoliated single- and few- to multilayer nanosheets among copious thick flakes over a centimeter/millimeter-size area is the first priority in their fundamental research and practical applications.

To date, many methods have been developed to identify the thickness of 2D nanosheets, such as atomic force microscopy (AFM), Raman spectroscopy, and optical microscopy (OM). Although AFM is commonly used to measure the thickness of 2D nanosheets, it is time-consuming and not suitable for rapid measurement over large area. In addition, AFM measurement might be affected by the absorbed water layer under 2D nanosheets or instrumental offset.[18,19] As a result, the thickness of single-layer graphene measured by AFM varied from 0.4 to 0.9 nm.[19−21] Raman spectroscopy is a quick characterization method to identify single- to few-layer 2D nanosheets.[12,17,22−24] However, the difference between double- and few-layer graphene or TMD nanosheets in Raman spectra is insufficient to accurately distinguish them.[4,22,23] Although low-frequency Raman spectroscopy (<50 cm^{-1}) has been used to reliably determine the layer number of graphene, MoS_2, or WSe_2,[12,17,24] it requires expensive and nonstandard equipment. On the contrary, OM is a simple, efficient, and nondestructive technique that enables rapid characterization of 2D nanosheets over a large area.[4,13,18,25−34] The OM method mainly relies on the optical contrast

* Address correspondence to hzhang@ntu.edu.sg.

Received for review September 10, 2013 and accepted October 16, 2013.

Published online October 16, 2013
10.1021/nn4047474

between a 2D nanosheet and the substrate for fast and unambiguous identification. To improve such contrast, several methods have been developed, including the use of narrow band illumination,[27,35] selection of optimal substrate,[25,29,35] collection of reflection spectra,[18] measurement of total color difference,[29] or ratio of color difference[28] *etc.* Unfortunately, these methods involve either special experimental setup or time-consuming image processing, and more importantly, they are not generalizable for identification of various kinds of nanosheets.

Here, we demonstrate a simple, rapid, and reliable method to identify 2D nanosheets (*e.g.*, graphene, MoS_2, WSe_2, and TaS_2) from single- to quindecuple-layer (1L−15L) without using any instrument or complex calculation. The contrast difference between the 2D nanosheet and substrate can be simply obtained from the brightness profile of their color images or grayscale images of the R, G, or B channel. The obtained values of contrast difference for nanosheets with different layer numbers can be plotted as a standard chart, based on which the layer number of a given nanosheet can be rapidly and accurately determined on the Si substrate coated with 90 or 300 nm SiO_2, referred to as 90 or 300 nm SiO_2/Si, respectively.

RESULTS AND DISCUSSION

Description of the Optical Identification Method. The key to the reliable and accurate optical identification of a 2D nanosheet is to correlate its layer number with its optical contrast with respect to the substrate. In our method, the optical contrast of a nanosheet (defined as C) and substrate (defined as C_S) was directly measured from its color optical image by using a free software (ImageJ). The contrast difference (defined as C_D) is obtained by subtracting C with C_S (eq 1). Similarly, for the grayscale image (from the R, G, or B channel), the contrast difference between the nanosheet and substrate (C_{DR}, C_{DG}, or C_{DB}) is calculated by subtracting the contrast of the nanosheet (C_R, C_G, or C_B) with that of the substrate (C_{SR}, C_{SG}, or C_{SB}) (eqs 2−4).

$$C_D = C - C_S \quad (1)$$

$$C_{DR} = C_R - C_{SR} \quad (2)$$

$$C_{DG} = C_G - C_{SG} \quad (3)$$

$$C_{DB} = C_B - C_{SB} \quad (4)$$

As a demonstration, Figure 1a shows the color optical image of a MoS_2 flake on 90 nm SiO_2/Si. Figure 1b is the contrast profile of the dashed rectangle highlighted in Figure 1a generated by ImageJ. The contrast values (C) of the octuple-layer (8L) and hextuple-layer (6L) MoS_2 nanosheets are 162.3 and 118.6, respectively, while the contrast value of 90 nm SiO_2/Si (C_S) is 120.4. According to eq 1, the contrast difference

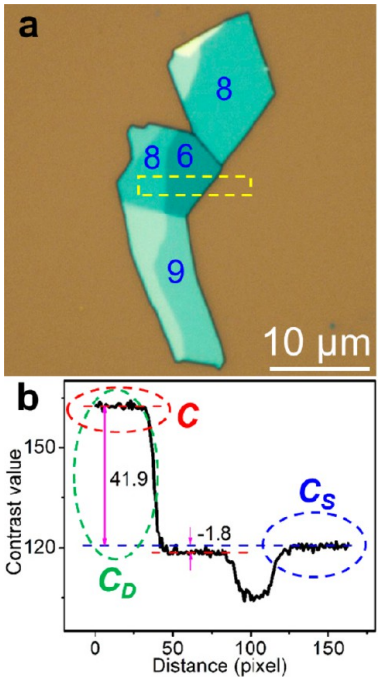

Figure 1. (a) Color optical image of a MoS_2 flake deposited on 90 nm SiO_2/Si. The digitals shown in (a) indicate the layer numbers of MoS_2 nanosheets, which were confirmed by AFM (Figure S1 in Supporting Information). (b) Contrast profile of the dashed rectangle shown in (a). C_S: contrast of 90 nm SiO_2/Si. C: contrast of MoS_2 nanosheet. C_D: the contrast difference between MoS_2 nanosheet and 90 nm SiO_2/Si.

between the 8L (or 6L) MoS_2 nanosheet and 90 nm SiO_2/Si substrate is calculated to be $C_D = 162.3 - 120.4 = 41.9$ (or $118.6 - 120.4 = -1.8$).

Optical Identification of 1L−15L Graphene Nanosheets on 90 and 300 nm SiO_2/Si. It has been reported that the color of a graphene nanosheet can be used to identify its thickness in combination with theoretical calculation.[29,33] Theoretical calculation predicted that SiO_2 film with thickness of 90 or 300 nm is the optimal dielectric layer for optical identification of graphene.[13,25,34] Here, thickness identification of 1L−15L graphene nanosheets on 90 or 300 nm SiO_2/Si can be achieved by our simple, rapid, and reliable method based on the measurement of optical contrast difference. Color optical images (Figure 2a−n), AFM measurement (Figure 2q), and Raman characterization (Figure S2 in Supporting Information (SI)) were first used to locate exfoliated graphene nanosheets on 90 nm SiO_2/Si and determine their thicknesses. After that, optical contrast differences (C_D) between 1L−15L graphene nanosheets and 90 nm SiO_2/Si were measured from their color optical images taken at different exposure times by using ImageJ (Figure 2o). It can be seen that, for 1L−15L graphene nanosheets, the absolute value of C_D increases with increasing exposure time from 20 to 140 ms and decreases from 160 to 300 ms. At 200 ms, as compared to other exposure times, such as 80 ms, the C_D values are mostly distinguishable among the 1L−15L nanosheets (Figure 2p

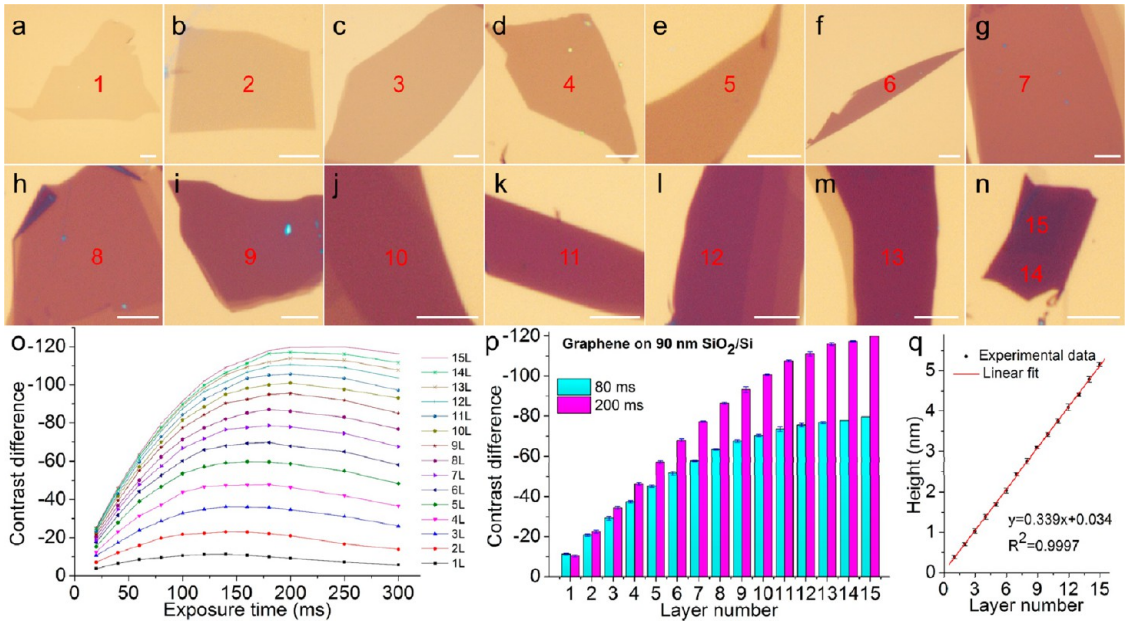

Figure 2. (a–n) Color optical images of 1L–15L graphene nanosheets on 90 nm SiO_2/Si. The scale bars shown in (a–n) are 10 μm. The digitals shown in (a–n) indicate the layer numbers of corresponding graphene nanosheets. (o) Plot of measured C_D values of 1L–15L graphene nanosheets on 90 nm SiO_2/Si at the exposure times of 20, 40, 60, 80, 100, 120, 140, 160, 180, 200, 250, and 300 ms. (p) Plot of measured C_D values of 1L–15L graphene nanosheets on 90 nm SiO_2/Si at the exposure times of 80 and 200 ms. (q) Thickness of 1L–15L graphene nanosheets measured by AFM.

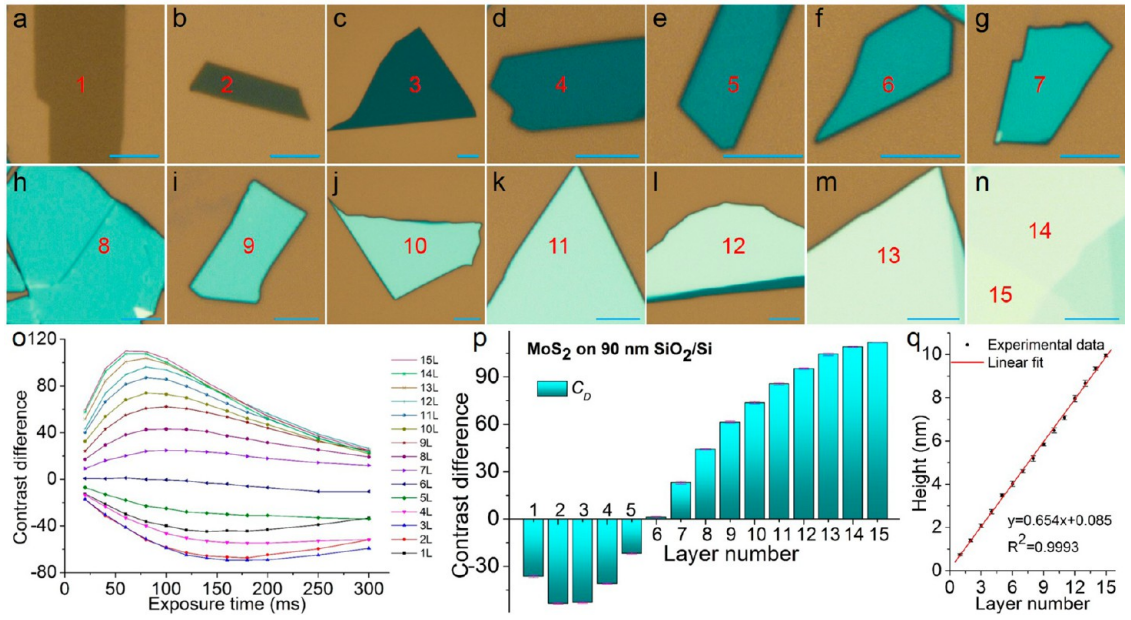

Figure 3. (a–n) Color optical images of 1L-15L MoS_2 nanosheets on 90 nm SiO_2/Si. The scale bar is 5 μm for each image. The digitals shown in (a–n) indicate the layer numbers of corresponding MoS_2 nanosheets. (o) Plot of measured C_D values of 1L–15L MoS_2 nanosheets on 90 nm SiO_2/Si at exposure times of 20, 40, 60, 80, 100, 120, 140, 160, 180, 200, 250, and 300 ms. (p) Plot of C_D values of 1L–15L MoS_2 on 90 nm SiO_2/Si at exposure time of 80 ms. (q) Thickness of 1L–15L MoS_2 nanosheets measured by AFM.

and Table S1 in SI), especially for those thicker than 10L. Therefore, a standard chart of C_D values at 200 ms for different layer numbers was generated (Figure 2p and Table S1 in SI), from which the thickness of a graphene nanosheet on 90 nm SiO_2/Si can be readily determined.

Similar to the C_D values, the C_{DR}, C_{DG}, and C_{DB} values of 1L–15L graphene nanosheets on 90 nm SiO_2/Si, measured from grayscale images of R, G, and B channels, respectively, can also be used for the layer number identification (Figure S3 and Table S1 in SI). Similarly, the C_D, C_{DR}, and C_{DG} values of 1L–13L graphene nanosheets on 300 nm SiO_2/Si can also be determined in the same manner and thus used for layer number identification of graphene (Figures S4 and S5 in SI).

Optical Identification of 1L−15L MoS_2 Nanosheets on 90 and 300 nm SiO_2/Si. As for the 1L−15L MoS_2 nanosheets on 90 nm SiO_2/Si (Figure 3a−n), they also show the thickness-dependent contrast difference at various exposure times (Figure 3o,p), confirmed by AFM measurement and low-frequency Raman characterization (Figure 3q and Figure S6 in SI). It is shown that at the exposure time of 80 ms, 5L−15L MoS_2 nanosheets are distinguishable based on C_D values (Figure 3o,p and Table S2 in SI). However, the C_D values of 1L−4L MoS_2 nanosheets are less differentiable, and especially the C_D values of 2L and 3L nanosheets are close, ∼−55 (Figure 3p and Figure 4a,b). In order to effectively distinguish 1L−4L MoS_2 nanosheets on 90 nm SiO_2/Si, the optical contrast differences measured from their grayscale images from R, G, and B channels (C_{DR}, C_{DG}, and C_{DB}) were used to determine their thicknesses (Figure 4c−i). As shown in Figure 4g−i, the C_{DB} values of 1L and 2L MoS_2 nanosheets are negative (1L, −26.4; 2L, −15.4), while those of 3L and 4L MoS_2 nanosheets are positive (3L, 4.2; 4L, 28.5). Meanwhile, the C_{DR} and C_{DG} values of 1L−4L MoS_2 nanosheets are also discrete enough for their thickness identification (Figure 4d,f,i). Therefore, 1L−15L MoS_2 nanosheets on 90 nm SiO_2/Si can be easily identified based on the measured C_D, C_{DR}, C_{DG}, and C_{DB} values.

An interesting feature was observed in the plot of C_D (or C_{DR}, C_{DG}, and C_{DB}) *versus* layer number of MoS_2. For example, there is a transition of C_D value between 5L and 6L nanosheets (Figure 3p and Table S2 in SI) from negative C_D at 5L (−21.8 ± 0.5) to positive C_D at 6L (1.0 ± 0.7). In other words, compared to the 90 nm SiO_2/Si substrate, 1L−5L MoS_2 nanosheets are darker while 6L−15L MoS_2 nanosheets are brighter under white light illumination. In this work, the thickness of a nanosheet with a minimum positive C_D value (similar for C_{DR}, C_{DG}, or C_{DB}) is defined as the transitional thickness (T_C). In this case, the T_C for MoS_2 nanosheets in color image and grayscale images of the R, G, and B channels is 6L, 10L, 5L, and 3L, respectively (Table 1). Therefore, the sign (positive or negative) of the C_D value enables the fast determination of the thickness range of a nanosheet (*i.e.*, below T_C or above T_C).

Similar to MoS_2 nanosheets on 90 nm SiO_2/Si, 1L−15L MoS_2 nanosheets on 300 nm SiO_2/Si can also be reliably identified by measuring the C_D value in combination with the C_{DR}, C_{DG}, and C_{DB} values (Figure 5a−o). The C_D values can be used to rapidly and reliably identify septuple-layer (7L) to 15L MoS_2 nanosheets but are less distinguishable among 1L−6L nanosheets (Figure 5n). In contrast to MoS_2 nanosheets on 90 nm SiO_2/Si (Figure 3), the transition of C_D occurs between 7L and 8L MoS_2 nanosheets on 300 nm SiO_2/Si, where 7L MoS_2 gives a negative C_D (−4.4 ± 0.2) and 8L MoS_2 gives a positive C_D (4.7 ± 0.3). The transition of C_D can be used as a mark to quickly determine a MoS_2 nanosheet thicker or thinner than 8L on 300 nm

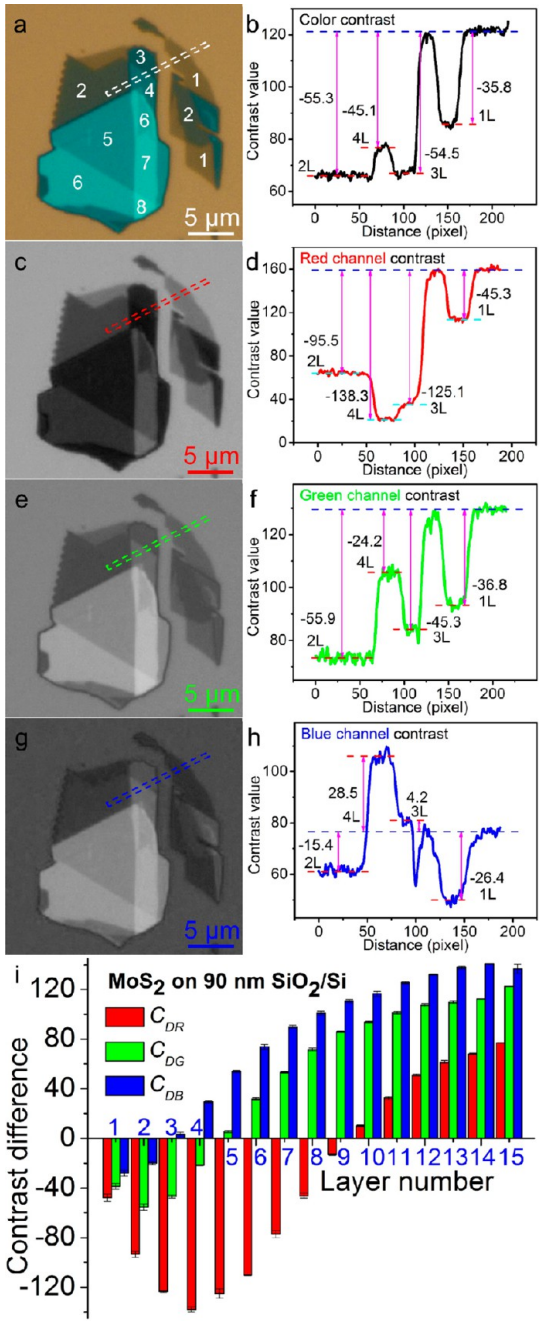

Figure 4. Color optical (a) and grayscale images of the (c) R, (e) G, and (g) B channels of MoS_2 flake on 90 nm SiO_2/Si. The digitals shown in (a) indicate the layer numbers of corresponding MoS_2 nanosheets. The corresponding contrast profiles of color optical (b) and grayscale images of the (d) R, (f) G, and (h) B channels of MoS_2 flake are obtained from the dashed rectangles shown in (a), (c), (e), and (g), respectively. (i) Plot of C_{DR}, C_{DG}, and C_{DB} values of 1L−15L MoS_2 nanosheets on 90 nm SiO_2/Si.

SiO_2/Si. Meanwhile, the C_{DR}, C_{DG}, and C_{DB} values are used to identify 1L−6L MoS_2 nanosheets, which are difficult to be distinguished by the measurement of C_D. For example, 1L−3L MoS_2 nanosheets can be differentiated by reading the C_{DR} values (Figure 5o and Table S2), whereas 4L−6L MoS_2 can be distinguished based on C_{DG} values (Figure 5o and Table S2).

TABLE 1. Transition Thickness of 2D Nanosheets with Minimum Positive Optical Contrast Difference on 90 and 300 nm SiO_2/Si

	90 nm SiO_2/Si				300 nm SiO_2/Si			
	C_D	C_{DR}	C_{DG}	C_{DB}	C_D	C_{DR}	C_{DG}	C_{DB}
graphene	$43L < T_C < 52L$[a]	$54L < T_C$[a]	$43L < T_C < 52L$[a]	$30L < T_C < 37L$[a]	$46L < T_C < 51L$[a]		~46L[a]	
MoS_2	6L	10L	5L	3L	8L	16L	4L	1L
WSe_2	7L	9L	7L	4L	8L	14L	5L	1L
TaS_2	27L	22L	25L	3L				

[a] See Figures S7 and S8 in SI for the detailed information.

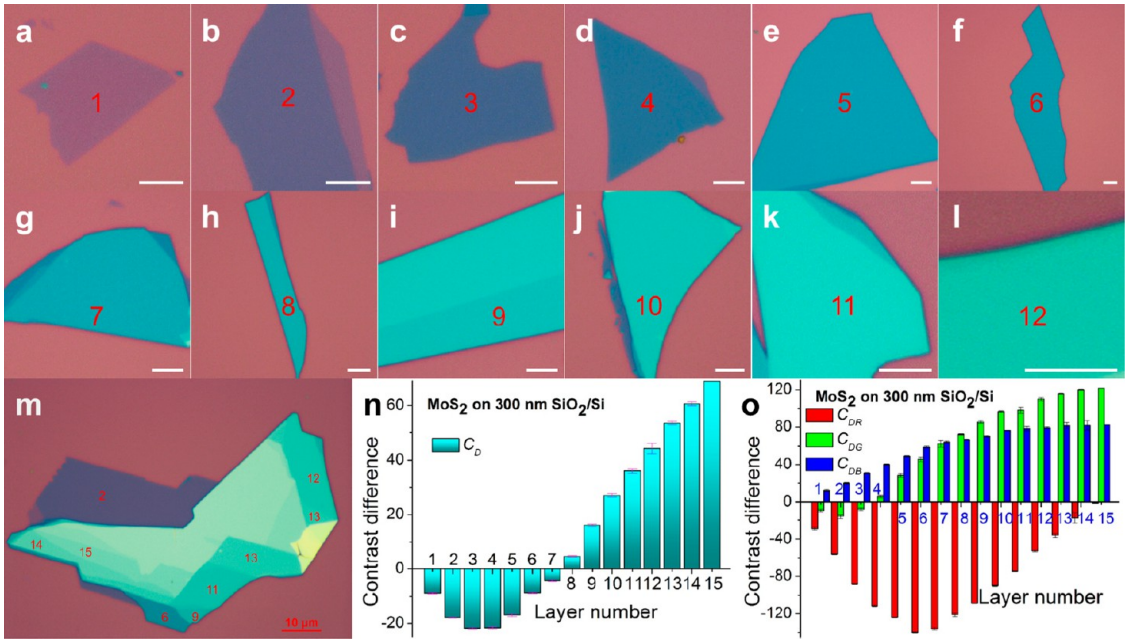

Figure 5. (a−m) Color optical images of 1L−15L MoS_2 on 300 nm SiO_2/Si. The scale bars are 5 μm for images a−l and 10 μm for image m. The digitals shown in (a−m) indicate the layer numbers of the corresponding MoS_2 nanosheets. Plots of (n) C_D values and (o) C_{DR}, C_{DG}, and C_{DB} values of 1L−15L MoS_2 nanosheets on 300 nm SiO_2/Si.

The T_C of C_{DG} is a 4L MoS_2 nanosheet (6.0 ± 1.3); that is, the C_{DG} values of 1L−3L MoS_2 nanosheets are negative while those of 4L−6L MoS_2 nanosheets are positive (see Table S2 in SI for detailed information). The highest absolute value of C_{DR} was found at the 6L MoS_2 nanosheet. After that, the absolute C_{DR} values of 7L−15L MoS_2 nanosheets decrease linearly with the thickness. Therefore, 1L−15L MoS_2 nanosheets on 300 nm SiO_2/Si can be readily identified using the C_D values in combination with the C_{DR} and C_{DG} values.

Optical Identification of Single- To Quattuordecuple-layer (1L−14L) WSe_2 Nanosheets on 90 and 300 nm SiO_2/Si. The optical contrast difference can also be used to identify 1L−14L WSe_2 nanosheets on 90 or 300 nm SiO_2/Si. Figure 6a−l shows the color optical images of 1L−14L WSe_2 nanosheets on 90 nm SiO_2/Si taken at the exposure time of 80 ms. The thickness of these nanosheets was confirmed by AFM measurement and low-frequency Raman spectra (Figure 6o and Figure S9 in SI). As shown in Figure 6m, the C_D values are distinguishable for 6L−14L WSe_2 nanosheets but are difficult to be differentiated for 1L−5L nanosheets. As shown in Figure 6m and Table S3 in SI, the 2L−4L WSe_2 nanosheets have similar C_D values (2L, −59.2 ± 1.4; 3L, −62.9 ± 1.5; 4L, −55.3 ± 1.4), so do 1L and 5L WSe_2 nanosheets (1L, −38.4 ± 1.7; 5L, −36.8 ± 2.4). In this case, the grayscale images of R, G and B channels were used to indicate the difference among the 1L−5L WSe_2 nanosheets (Figure 6n). By comparing C_{DR}, C_{DG}, and C_{DB} values at various layer numbers, it was found that the C_{DR} values combined with C_{DB} values are mostly suitable to rapidly differentiate 1L−5L WSe_2 nanosheets because of the sufficient gap between the C_{DR} and C_{DB} values of adjacent layer numbers (Table S3 in SI). The C_{DB} value of 1L WSe_2 nanosheet is negative (−27.6 ± 1.4), while that of 5L WSe_2 nanosheet is positive (16.7 ± 0.9). In addition, the T_C of C_{DB} values is the 4L WSe_2 nanosheet (0.3 ± 0.8). Thus 1L, 4L, and 5L WSe_2 nanosheets can be easily identified by reading the C_{DB} values. Although 2L and 3L WSe_2 nanosheets have similar C_{DG} values (2L, −76.8 ± 1.4; 3L, −76.5 ± 1.9), their C_{DR} values (2L, −80.0 ± 0.9; 3L, −103.0 ± 0.4) are fairly discrete for

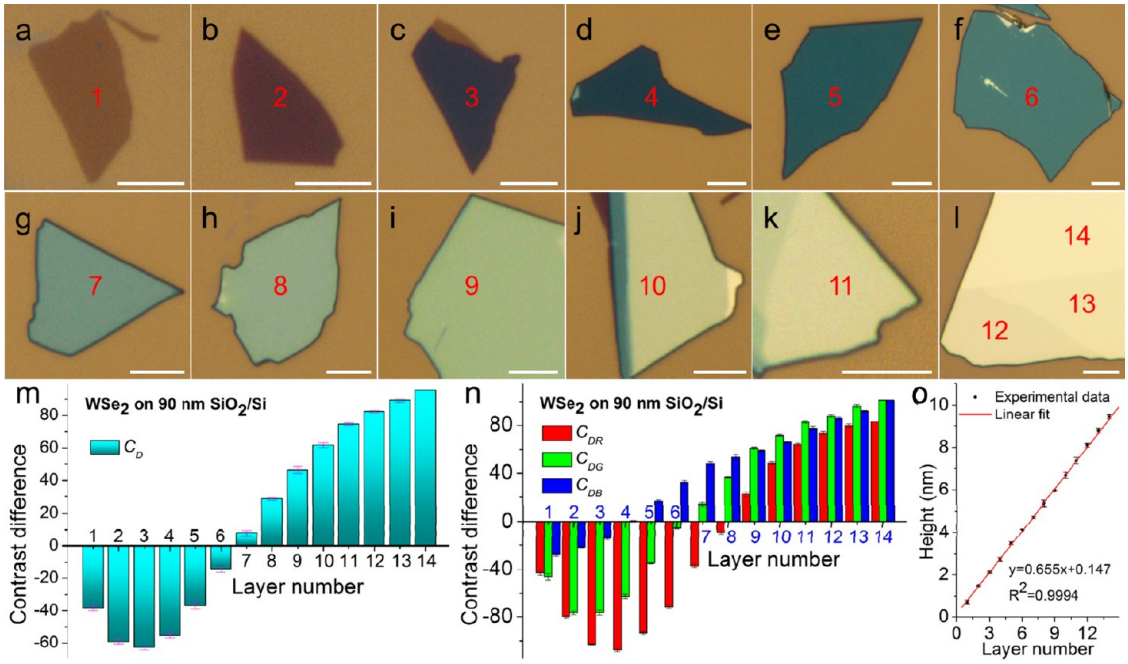

Figure 6. (a−l) Color optical images of 1L−14L WSe_2 nanosheets on 90 nm SiO_2/Si. The scale bars shown in (a−l) are 5 μm. The digitals shown in (a−l) indicate the layer numbers of corresponding WSe_2 nanosheets. Plots of (m) C_D and (n) C_{DR}, C_{DG}, and C_{DB} values of 1L−14L WSe_2 nanosheets on 90 nm SiO_2/Si at the exposure time of 80 ms. (o) Thickness of 1L−14L WSe_2 nanosheets measured by AFM.

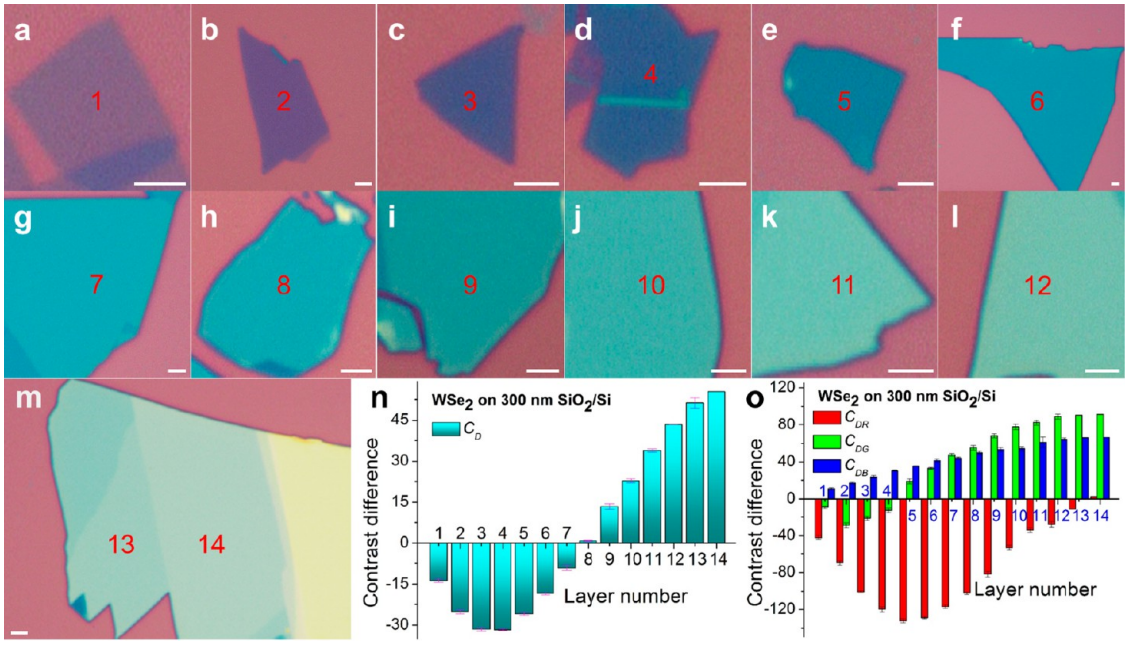

Figure 7. (a−m) Color optical images of 1L−14L WSe_2 on 300 nm SiO_2/Si. The scale bars shown in (a−m) are 2 μm. The digitals shown in (a−m) indicate the layer numbers of the corresponding WSe_2 nanosheets. Plots of (n) C_D values and (o) C_{DR}, C_{DG}, and C_{DB} values of 1L−14L WSe_2 nanosheets on 300 nm SiO_2/Si.

thickness identification. Thus, 1L−14L WSe_2 nanosheets on 90 nm SiO_2/Si can be readily identified using the C_D values in combination with C_{DR} and C_{DB} values. Furthermore, for 1L−14L WSe_2 nanosheets on 300 nm SiO_2/Si, their C_D, C_{DR}, C_{DG}, and C_{DB} values are also distinguishable for fast thickness determination (Figure 7 and Table S3 in SI). In this case, the T_C of C_D is 8L (Table 1 and Table S3 in SI) and the C_D values of 8L−14L WSe_2 can be used to rapidly and reliably distinguish them (Figure 7n). As for 1L−7L WSe_2 nanosheets, the C_{DR}, C_{DG}, and C_{DB} values are used to determine their thicknesses (Table S3 in SI and Figure 7o). Therefore, 1L−14L WSe_2 nanosheets on 300 nm SiO_2/Si can be readily identified using the C_D values in combination with the C_{DR} and C_{DG} values.

Verification of Layer Number Identification of Graphene, MoS_2, and WSe_2 Nanosheets on 90 nm SiO_2/Si. In order to verify the accuracy of our optical method, the thicknesses of mechanically exfoliated graphene, MoS_2, and WSe_2 nanosheets on 90 nm SiO_2/Si were first identified using the measurement of C_D values followed by AFM measurement to confirm it.

With graphene as an example, Figure 8a shows the color optical image of a graphene nanosheet. As shown in Figure 8b, the C_D values measured from the red dashed rectangle shown in Figure 8a are −10.7, −57.6, and −68.3. According to the standard chart shown in Figure 2o,p and Table S1 in SI, these C_D values correspond to 1L, 5L, and 6L graphene nanosheets, respectively. AFM measurement on these regions show thicknesses of 0.4, 1.7, and 2.1 nm (Figure 8c,d), respectively, consistent with the thickness of 1L, 5L, and 6L graphene (Figure 2q and Table S4 in SI), confirming the accuracy of the optical identification result.

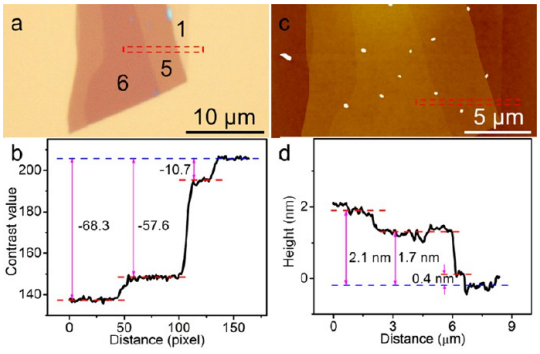

Figure 8. Color optical (a) and AFM height (c) images of graphene flake on 90 nm SiO_2/Si. The corresponding contrast difference (b) and height (d) profiles are obtained from the dashed rectangles shown in (a) and (c), respectively. The digitals shown in (a) indicate the layer numbers of corresponding graphene nanosheets.

As for MoS_2, Figure 9a shows the color optical image of an exfoliated MoS_2 nanosheet, displaying three distinct color regions. C_D values measured from the red dashed rectangle shown in Figure 9a are −2.5, 22.4, and 60.3, which correspond, respectively, to 6L, 7L, and 9L MoS_2 nanosheets according to the standard chart shown in Figure 3o,p and Table S2 in SI. The corresponding thicknesses of the these three regions measured by AFM (Figure 9c,d) are 4.1, 4.7, and 5.9 nm, respectively, consistent with those of 6L, 7L, and 9L MoS_2 nanosheets.

Similarly, for the optical identification of WSe_2 nanosheet, C_D values of 9.5 and 30.8 (Figure 9f) were first obtained from two different color regions (highlighted in the red dashed rectangle shown in Figure 9e), corresponding to 7L and 8L WSe_2 nanosheets, respectively, by referring to the standard chart shown in Figure 6m and Table S3 in SI. AFM measurement (Figure 9g,h) on these two regions indicates thicknesses of 4.7 and 5.4 nm, respectively, in agreement with those of 7L and 8L WSe_2 nanosheets (Figure 6o and Table S4 in SI).

Besides graphene, MoS_2 and WSe_2 nanosheets, our method can also be used for the rapid and reliable identification of TaS_2 nanosheets on 90 nm SiO_2/Si. The C_D values of 2L−8L and 15L to octoviguple-layer (28L) and duotriguple-layer (32L) TaS_2 nanosheets are discrete enough for reliable identification (Table S5 and Figure S10 in SI). In combination with the C_{DR}, C_{DG}, and C_{DB} values (Table S5 in SI), 2L−28L and 32L TaS_2 nanosheets can be easily and reliably identified (Figures S10 and S11 in SI), indicating the generalizability of our method in the thickness identification of 2D nanosheets.

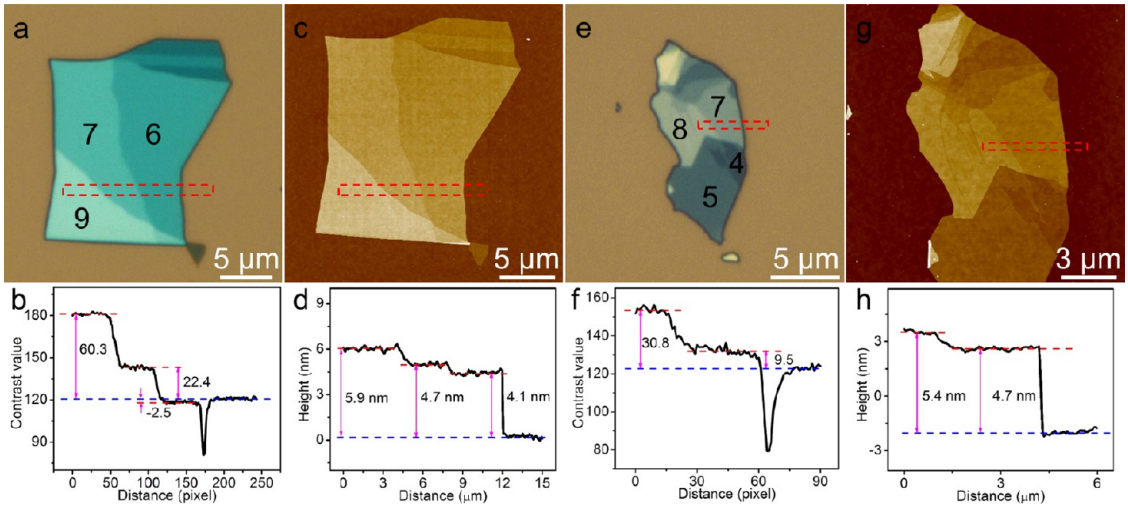

Figure 9. Color optical images of MoS_2 (a) and WSe_2 (e) nanosheets on 90 nm SiO_2/Si and the corresponding contrast profiles (b,f) obtained from the dashed rectangles in (a) and (e), respectively. AFM height images of MoS_2 (c) and WSe_2 (g) nanosheets on 90 nm SiO_2/Si, and the corresponding height profiles (d,h) obtained from the dashed rectangles in (c) and (g), respectively. The digitals shown in (a) and (e) indicate the layer numbers of corresponding MoS_2 and WSe_2 nanosheets, respectively.

The measurement of C_D is affected by the intensity of illumination, thickness of SiO_2 film, and exposure time. In this work, the exposure time is fixed. Therefore, the measurement error may arise from the thickness variation of commercial SiO_2 film and fluctuation of illumination intensity, which is manually adjusted in our optical microscope (Figure S12 in SI). Take 6L MoS_2 as an example; the C_D value of 6L MoS_2 is 1.0 ± 0.7 (Figure 3p and Table S2 in SI) when the 90 nm SiO_2/Si substrate (12 mm × 12 mm) cut from the same wafer was used. However, the C_D values of 6L MoS_2 nanosheets shown in Figure 1a and Figure 9a are −1.8 and −2.5, respectively, when the 90 nm SiO_2/Si substrate (12 mm × 12 mm) cut from another wafer was used. Nevertheless, we found that the C_D value variation of MoS_2 nanosheets on different wafers is usually smaller than 3, which is much smaller than the difference of C_D values between the adjacent layers. In other words, the difference among C_D values is sufficient for thickness determination. In addition, the transition thickness (T_C) of optical contrast difference is related to the type of material, the thickness of SiO_2 film, as well as the color of optical image. As shown in Table 1, the T_C values of C_D, C_{DR}, C_{DG}, and C_{DB} follow the order of $C_{DR} > C_D \geq C_{DG} > C_{DB}$ for 1L−15L MoS_2 and 1L−14L WSe_2 nanosheets on 90 and 300 nm SiO_2/Si. In the case of TaS_2 nanosheets on 90 nm SiO_2/Si, the T_C values of C_D, C_{DR}, and C_{DG} follow the order of $C_D > C_{DG} > C_{DR}$ (Table 1). In terms of graphene nanosheets on 90 and 300 nm SiO_2/Si, the T_C values of C_D, C_{DR}, C_{DG}, and C_{DB} are much larger compared to those of MoS_2, WSe_2, and TaS_2 nanosheets (Table 1 and Figures S7 and S8). The variation of T_C for different materials might be attributed to their intrinsic properties, such as refractive index.

CONCLUSION

In summary, a universal optical method has been developed for simple, rapid, and reliable identification of 1L−15L 2D nanosheets, including graphene, MoS_2, WSe_2, and TaS_2, on 90 and 300 nm SiO_2/Si. By processing the color optical images and the grayscale images of R, G, and B channels, the optical contrast differences between 2D nanosheets and SiO_2/Si were measured using ImageJ and plotted as standard charts to guide the layer number identification. The transition of C_D, C_{DR}, C_{DG}, and C_{DB} values can be used as a clear mark for quick identification of layer number. Neither complex calculation nor special instrument is required in our method, making it applicable for any laboratories equipped with a standard optical microscope and digital camera. Our simple optical identification method will facilitate the fundamental study and practical applications of 2D nanomaterials and accelerate their progress toward future commercialization. Furthermore, our method potentially expands the capability of optical microscopy in the study of nanomaterials and applications of nanotechnology.

METHODS AND MATERIALS

Mechanical Exfoliation of 2D Nanosheets (Graphene, MoS_2, WSe_2, and TaS_2 Nanosheets). Natural graphite (NGS Naturgraphit GmbH, Germany), MoS_2 crystals (SPI Supplies, USA), WSe_2, and TaS_2 crystals (Nanoscience Instruments, Inc., USA) were used for preparation of mechanically exfoliated 2D nanosheets, which then were deposited onto the freshly cleaned 90 and 300 nm SiO_2-coated Si substrates (90 and 300 nm SiO_2/Si).

Capture of Optical Images of 2D Nanosheets. The bright-field optical microscope (Eclipse LV100D with a 100×, 0.9 numerical aperture (NA) objective, Nikon) was used to locate and image the 2D nanosheets. A lamphouse (LV-LH50PC) equipped with high-intensity halogen lamp (12 V, 50 W) was used as the light source. The intensity of the light source was adjusted by turning the brightness control knob to level 9 (Figure S12 in SI). For graphene and MoS_2 nanosheets on 90 nm SiO_2/Si, the optical images were captured at the exposure times of 20, 40, 60, 80, 100, 120, 140, 160, 180, 200, 250, and 300 ms. For WSe_2 and TaS_2 nanosheets on 90 nm SiO_2/Si, the optical images were captured at the exposure time of 80 ms. For various 2D nanosheets on 300 nm SiO_2/Si, the optical images were captured at the exposure time of 50 ms. A DS camera head (DS-Fi1) with a digital camera control unit (DS-U3) was used to capture color optical images of 2D nanosheets at the resolution of 1280 × 960 pixels. The imaging software is NIS-Elements F (version 4.00.06), and the white balance is calibrated as R/B = 1.23:1.24 (Figure S12 in SI). In order to give quantitative and statistic characterization of the layer numbers of 2D nanosheets, a large amount of graphene, MoS_2, WSe_2, and TaS_2 flakes with layer numbers ranged from 1L to 32L, prepared by the mechanical cleavage technique, was imaged by optical microscopy and analyzed by using our optical method. For 1L to 10L 2D nanosheets, at least five samples were collected for measurement. For 2D nanosheets thicker than 11L, usually three samples were collected for measurement.

Optical Contrast Difference Measurement of Color Optical Images and Grayscale Images of R, G, and B Channels by Using ImageJ. The color optical images of 2D nanosheets were processed by the ImageJ (version 1.46p, National Institutes of Health, USA). For the color image (RGB image), the contrast value of each pixel (C_V), that is, brightness value, is calculated using the following equation

$$C_V = (C_{VR} + C_{VG} + C_{VB})/3 \quad (5)$$

where C_{VR}, C_{VG}, and C_{VB} are the R, G, and B values per pixel in color image, respectively; 0 is darkest, and 255 is brightest.

The grayscale images of R, G, and B channels were extracted by using the "Split Channels" command from "Image > Color > Split Channels" in the menu bar, where 0 is darkest and 255 is brightest. In the color or grayscale image, we can drag the left button of the mouse to draw a rectangular box across the 2D nanosheet and then press "K" to obtain the contrast profile of the selected area. In the plot of contrast profile, click "List" to show the contrast values of the 2D nanosheet and SiO_2 substrate.

The detailed optical contrast difference (C_D, C_{DR}, C_{DG}, and C_{DB}) values of 2D nanosheets are listed in Tables S1−S4 in SI.

Thickness Measurement of 2D Nanosheets by AFM. AFM (Dimension ICON with NanoScope V controller, Bruker, USA) was used to confirm the layer number of 2D nanosheets by measuring the film thickness in tapping mode in air. The thickness values of 2D nanosheets are listed in Table S4 in SI.

Raman Measurement of 2D Nanosheets. Analysis of the MoS_2 and WSe_2 nanosheets by low-frequency Raman spectroscopy was carried out at room temperature using a micro-Raman spectrometer (Horiba-JY T64000) equipped with a liquid-nitrogen-cooled

charge-coupled device. The measurements were conducted in a backscattering configuration excited with a solid-state green laser (λ = 532 nm). A reflecting Bragg grating (OptiGrate) followed by another ruled reflecting grating was used to filter the laser side bands, as such ~8 cm^{-1} limit of detection was achieved using most solid-state or gas laser lines. All spectra were collected through a 100× objective and dispersed by a 1800 g/mm grating under a triple subtractive mode with a spectra resolution of 1 cm^{-1}. The Raman spectra were calibrated by using the peak of Si substrate (520 cm^{-1}). The laser power at the sample surface was less than 1.5 mW for MoS_2 and 0.3 mW for WSe_2.

Analysis of graphene nanosheets by Raman spectroscopy was carried out on a WITec CRM200 confocal Raman microscopy system with the excitation line of 488 nm and an air cooling charge-coupled device (CCD) as the detector (WITec Instruments Corp., Germany).

Conflict of Interest: The authors declare no competing financial interest.

Acknowledgment. This work was supported by AcRF Tier 1 (RG 61/12) and Start-Up Grant (M4080865.070.706022) in Singapore. This research is also funded by the Singapore National Research Foundation, and the publication is supported under the Campus for Research Excellence and Technological Enterprise (CREATE) programme (Nanomaterials for Energy and Water Management).

Supporting Information Available: AFM measurement of MoS_2 flake shown in Figure 1a. Raman spectra of 1L−15L graphene, MoS_2, and WSe_2 nanosheets. Contrast difference plot of 1L−15L graphene on 90 nm SiO_2/Si. Optical images and contrast difference plots of 1L−15L graphene on 300 nm SiO_2/Si. The detailed optical contrast difference (C_D, C_{DR}, C_{DG}, and C_{DB}) and height values of 2D nanosheets. Optical images and contrast difference plots of 2L−28L and 32L TaS_2 nanosheets on 90 nm SiO_2/Si. This material is available free of charge *via* the Internet at http://pubs.acs.org.

REFERENCES AND NOTES

1. Chhowalla, M.; Shin, H. S.; Eda, G.; Li, L. J.; Loh, K. P.; Zhang, H. The Chemistry of Two-Dimensional Layered Transition Metal Dichalcogenide Nanosheets. *Nat. Chem.* **2013**, *5*, 263–275.
2. Huang, X.; Yin, Z. Y.; Wu, S. X.; Qi, X. Y.; He, Q. Y.; Zhang, Q. C.; Yan, Q. Y.; Boey, F.; Zhang, H. Graphene-Based Materials: Synthesis, Characterization, Properties, and Applications. *Small* **2011**, *7*, 1876–1902.
3. Li, H.; Lu, G.; Wang, Y.; Yin, Z. Y.; Cong, C.; He, Q.; Wang, L.; Ding, F.; Yu, T.; Zhang, H. Mechanical Exfoliation and Characterization of Single- and Few-Layer Nanosheets of WSe_2, TaS_2, and $TaSe_2$. *Small* **2013**, *9*, 1974–1981.
4. Li, H.; Lu, G.; Yin, Z. Y.; He, Q. Y.; Li, H.; Zhang, Q.; Zhang, H. Optical Identification of Single- and Few-Layer MoS_2 Sheets. *Small* **2012**, *8*, 682–686.
5. Li, H.; Yin, Z. Y.; He, Q. Y.; Li, H.; Huang, X.; Lu, G.; Fam, D. W. H.; Tok, A. I. Y.; Zhang, Q.; Zhang, H. Fabrication of Single- and Multilayer MoS_2 Film-Based Field-Effect Transistors for Sensing NO at Room Temperature. *Small* **2012**, *8*, 63–67.
6. Wang, Q. H.; Kalantar-Zadeh, K.; Kis, A.; Coleman, J. N.; Strano, M. S. Electronics and Optoelectronics of Two-Dimensional Transition Metal Dichalcogenides. *Nat. Nanotechnol.* **2012**, *7*, 699–712.
7. Yin, Z. Y.; Li, H.; Li, H.; Jiang, L.; Shi, Y. M.; Sun, Y. H.; Lu, G.; Zhang, Q.; Chen, X. D.; Zhang, H. Single-Layer MoS_2 Phototransistors. *ACS Nano* **2012**, *6*, 74–80.
8. Coleman, J. N.; Lotya, M.; O'Neill, A.; Bergin, S. D.; King, P. J.; Khan, U.; Young, K.; Gaucher, A.; De, S.; Smith, R. J.; *et al.* Two-Dimensional Nanosheets Produced by Liquid Exfoliation of Layered Materials. *Science* **2011**, *331*, 568–571.
9. Radisavljevic, B.; Radenovic, A.; Brivio, J.; Giacometti, V.; Kis, A. Single-Layer MoS_2 Transistors. *Nat. Nanotechnol.* **2011**, *6*, 147–150.
10. Zeng, Z. Y.; Yin, Z. Y.; Huang, X.; Li, H.; He, Q. Y.; Lu, G.; Boey, F.; Zhang, H. Single-Layer Semiconducting Nanosheets: High-Yield Preparation and Device Fabrication. *Angew. Chem., Int. Ed.* **2011**, *50*, 11093–11097.
11. Li, H.; Qi, X. Y.; Wu, J.; Zeng, Z. Y.; Wei, J.; Zhang, H. Investigation of MoS_2 and Graphene Nanosheets by Magnetic Force Microscopy. *ACS Nano* **2013**, *7*, 2842–2849.
12. Tan, P. H.; Han, W. P.; Zhao, W. J.; Wu, Z. H.; Chang, K.; Wang, H.; Wang, Y. F.; Bonini, N.; Marzari, N.; Pugno, N.; *et al.* The Shear Mode of Multilayer Graphene. *Nat. Mater.* **2012**, *11*, 294–300.
13. Nolen, C. M.; Denina, G.; Teweldebrhan, D.; Bhanu, B.; Balandin, A. A. High-Throughput Large-Area Automated Identification and Quality Control of Graphene and Few-Layer Graphene Films. *ACS Nano* **2011**, *5*, 914–922.
14. Kim, S.; Konar, A.; Hwang, W. S.; Lee, J. H.; Lee, J.; Yang, J.; Jung, C.; Kim, H.; Yoo, J. B.; Choi, J. Y.; *et al.* High-Mobility and Low-Power Thin-Film Transistors Based on Multilayer MoS_2 Crystals. *Nat. Commun.* **2012**, *3*, 1011.
15. Das, S.; Chen, H. Y.; Penumatcha, A. V.; Appenzeller, J. High Performance Multilayer MoS_2 Transistors with Scandium Contacts. *Nano Lett.* **2013**, *13*, 100–105.
16. Lee, H. S.; Min, S. W.; Chang, Y. G.; Park, M. K.; Nam, T.; Kim, H.; Kim, J. H.; Ryu, S.; Im, S. MoS_2 Nanosheet Phototransistors with Thickness-Modulated Optical Energy Gap. *Nano Lett.* **2012**, *12*, 3695–3700.
17. Zhao, Y. Y.; Luo, X.; Li, H.; Zhang, J.; Araujo, P. T.; Gan, C. K.; Wu, J.; Zhang, H.; Quek, S. Y.; Dresselhaus, M. S.; *et al.* Inter Layer Breathing and Shear Modes in Few-Trilayer MoS_2 and WSe_2. *Nano Lett.* **2013**, *13*, 1007–1015.
18. Ni, Z. H.; Wang, H. M.; Kasim, J.; Fan, H. M.; Yu, T.; Wu, Y. H.; Feng, Y. P.; Shen, Z. X. Graphene Thickness Determination Using Reflection and Contrast Spectroscopy. *Nano Lett.* **2007**, *7*, 2758–2763.
19. Xu, K.; Cao, P. G.; Heath, J. R. Graphene Visualizes the First Water Adlayers on Mica at Ambient Conditions. *Science* **2010**, *329*, 1188–1191.
20. Koh, Y. K.; Bae, M. H.; Cahill, D. G.; Pop, E. Reliably Counting Atomic Planes of Few-Layer Graphene (n > 4). *ACS Nano* **2011**, *5*, 269–274.
21. Cheng, Z. G.; Zhou, Q. Y.; Wang, C. X.; Li, Q. A.; Wang, C.; Fang, Y. Toward Intrinsic Graphene Surfaces: A Systematic Study on Thermal Annealing and Wet-Chemical Treatment of SiO_2-Supported Graphene Devices. *Nano Lett.* **2011**, *11*, 767–771.
22. Lee, C.; Yan, H.; Brus, L. E.; Heinz, T. F.; Hone, J.; Ryu, S. Anomalous Lattice Vibrations of Single- and Few-Layer MoS_2. *ACS Nano* **2010**, *4*, 2695–2700.
23. Hao, Y. F.; Wang, Y. Y.; Wang, L.; Ni, Z. H.; Wang, Z. Q.; Wang, R.; Koo, C. K.; Shen, Z. X.; Thong, J. T. L. Probing Layer Number and Stacking Order of Few-Layer Graphene by Raman Spectroscopy. *Small* **2010**, *6*, 195–200.
24. Zhang, X.; Han, W. P.; Wu, J. B.; Milana, S.; Lu, Y.; Li, Q. Q.; Ferrari, A. C.; Tan, P. H. Raman Spectroscopy of Shear and Layer Breathing Modes in Multilayer MoS_2. *Phys. Rev. B* **2013**, *87*, 115413.
25. Blake, P.; Hill, E. W.; Neto, A. H. C.; Novoselov, K. S.; Jiang, D.; Yang, R.; Booth, T. J.; Geim, A. K. Making Graphene Visible. *Appl. Phys. Lett.* **2007**, *91*, 063124.
26. Gaskell, P. E.; Skulason, H. S.; Rodenchuk, C.; Szkopek, T. Counting Graphene Layers on Glass *via* Optical Reflection Microscopy. *Appl. Phys. Lett.* **2009**, *94*, 143101.
27. Castellanos-Gomez, A.; Agrait, N.; Rubio-Bollinger, G. Optical Identification of Atomically Thin Dichalcogenide Crystals. *Appl. Phys. Lett.* **2010**, *96*, 213116.
28. Chen, Y. F.; Liu, D.; Wang, Z. G.; Li, P. J.; Hao, X.; Cheng, K.; Fu, Y.; Huang, L. X.; Liu, X. Z.; Zhang, W. L.; *et al.* Rapid Determination of the Thickness of Graphene Using the Ratio of Color Difference. *J. Phys. Chem. C* **2011**, *115*, 6690–6693.
29. Gao, L. B.; Ren, W. C.; Li, F.; Cheng, H. M. Total Color Difference for Rapid and Accurate Identification of Graphene. *ACS Nano* **2008**, *2*, 1625–1633.
30. Wang, Y. Y.; Gao, R. X.; Ni, Z. H.; He, H.; Guo, S. P.; Yang, H. P.; Cong, C. X.; Yu, T. Thickness Identification of

Two-Dimensional Materials by Optical Imaging. *Nanotechnology* **2012**, *23*, 495713.
31. Late, D. J.; Liu, B.; Matte, H. S. S. R.; Rao, C. N. R.; Dravid, V. P. Rapid Characterization of Ultrathin Layers of Chalcogenides on SiO_2/Si Substrates. *Adv. Funct. Mater.* **2012**, *22*, 1894–1905.
32. Jung, I.; Pelton, M.; Piner, R.; Dikin, D. A.; Stankovich, S.; Watcharotone, S.; Hausner, M.; Ruoff, R. S. Simple Approach for High-Contrast Optical Imaging and Characterization of Graphene-Based Sheets. *Nano Lett.* **2007**, *7*, 3569–3575.
33. Roddaro, S.; Pingue, P.; Piazza, V.; Pellegrini, V.; Beltram, F. The Optical Visibility of Graphene: Interference Colors of Ultrathin Graphite on SiO_2. *Nano Lett.* **2007**, *7*, 2707–2710.
34. Casiraghi, C.; Hartschuh, A.; Lidorikis, E.; Qian, H.; Harutyunyan, H.; Gokus, T.; Novoselov, K. S.; Ferrari, A. C. Rayleigh Imaging of Graphene and Graphene Layers. *Nano Lett.* **2007**, *7*, 2711–2717.
35. Benameur, M. M.; Radisavljevic, B.; Heron, J. S.; Sahoo, S.; Berger, H.; Kis, A. Visibility of Dichalcogenide Nanolayers. *Nanotechnology* **2011**, *22*, 125706.